Catal Lett (2008) 124:39–45
DOI 10.1007/s10562-008-9505-6

Promotional Effects of H_2O Treatment on NO_x Storage Over Fresh and Thermally Aged Pt–BaO/Al_2O_3 Lean NO_x Trap Catalysts

Do Heui Kim · Ya-Huei Chin · Ja Hun Kwak · Charles H. F. Peden

Received: 24 March 2008 / Accepted: 23 April 2008 / Published online: 17 May 2008

Abstract A simple liquid water treatment applied to fresh and thermally aged Pt(2 wt%)–BaO(20 wt%)/Al_2O_3 lean NO_x trap catalysts at room temperature induces morphological and structural changes in the barium species as followed by XRD and TEM analysis. During the water treatment, liquid water sufficient to fill the catalyst pore volume is brought into contact with the samples. It was found that irrespective of the original barium chemical state (highly dispersed BaO or crystalline $BaAl_2O_4$), exposing the sample to this liquid water treatment promotes the formation of $BaCO_3$ crystallites (about 15–25 nm of its size) without changing the Pt particle size. Such transformations of the barium species are found to significantly promote NO_x uptake from 250 to 450 °C. The increase in the NO_x uptake for the water-treated samples can be attributed to an enhanced Pt–Ba interaction through the redistribution of barium species. These results provide useful information for the regeneration of aged lean NO_x trap catalysts since water is plentiful in the exhaust of diesel or lean-burn engines.

Keywords Pt–BaO/Al_2O_3 · Lean NO_x trap catalyst · Water treatment · $BaAl_2O_4$

D. H. Kim (✉) · Y.-H. Chin · J. H. Kwak · C. H. F. Peden
Institute for Interfacial Catalysis, Pacific Northwest National Laboratory, P.O. Box 999, Richland, WA 99352, USA
e-mail: do.kim@pnl.gov

Present Address:
Y.-H. Chin
Department of Chemical Engineering, University of California, Berkeley, CA, USA

1 Introduction

Diesel vehicles are getting more attention globally due to their higher fuel efficiency and correspondingly lower emission of greenhouse gases than gasoline-powered automobiles. However, the conventional three-way catalyst (TWC) does not remove NO_x (nitrogen oxides) emissions efficiently from diesel engine exhaust because this exhaust contains excess oxygen (lean atmosphere). A lot of research has been aimed at identifying appropriate technologies for the removal of NO_x under these highly oxidizing conditions ($\sim$10 vol% O_2), with the lean NO_x trap (LNT) technology being regarded as one of the more promising solutions [1]. The LNT catalyst, consisting of precious metal (Pt) and alkaline earth metal (Ba) on an Al_2O_3 support material, is operated under continuous lean-rich cycles, so it stores NO_x in a nitrate form (typically, barium nitrate) during the lean cycle and reduces the stored nitrates during a subsequent fuel rich cycle [2].

However, there is a critical deactivation issue that arises from the presence of low levels of SO_2 in the diesel exhaust (about 10–20 ppm) [3, 4]. Similar to NO, SO_2 undergoes chemical conversion on the catalyst and is eventually stored as $BaSO_4$. Formation of $BaSO_4$, a thermodynamically more stable phase than $Ba(NO_3)_2$, BaO, or $BaCO_3$ [5], decreases the available barium sites for NO_x storage, eventually leading to the deactivation of the catalyst. Therefore, a high temperatures de-sulfation process to convert $BaSO_4$ back into BaO or $BaCO_3$ is required for regeneration of the catalyst. During this de-sulfation process, several effects of thermal aging, such as Pt sintering, loss of Al_2O_3 surface area, and formation a of less-reactive $BaAl_2O_4$ phase, have been reported on this class of LNT catalysts [6, 7]. Pt sintering is detrimental because it reduces the interaction between the Pt and Ba phases, with

such an interaction likely important for efficient operation during the lean cycle for the transfer of NO_2, formed over Pt sites, to vicinal barium sites for storage [8]. Meanwhile, Li, et al. [9] at Ford have reported that the formation of $BaAl_2O_4$ directly leads to a decrease in the number of active Ba sites and, thus, a loss of the available storage sites. On the other hand, Hodjati et al. [10, 11] observed improved NO_x storage performance with $BaAl_2O_4$ compared to BaO and/or $BaCO_3$, attributed to its lack of interaction with CO_2, suggesting that a $BaAl_2O_4$ phase should active for the trapping of NO_x. Still, $BaAl_2O_4$ formation may also reduce the contact between Pt and Ba phases.

Once formed during high temperature treatment, Graham et al. [12] observed that $BaAl_2O_4$ will undergo an interesting phase transformation to crystalline $BaCO_3$ upon H_2O treatment. In addition, our group [13] found that not only $BaAl_2O_4$, but also other Ba phases (e.g., $BaCO_3$ and BaO), are able to transform to bulk $BaCO_3$ during H_2O treatment at room temperature via a so-called carbonation reaction. This process turns out to be largely dependent on the presence of liquid water within the sample, where dissolution of gaseous CO_2 to form carbonic acid (CO_3^{2-}) occurs continuously and results in the formation of large $BaCO_3$ crystallites via the carbonation reaction that is, in turn, initiated by Ba dissolution. Although Graham et al. [12] showed a decrease in the NO_x uptake after a H_2O treatment was performed on a fresh Pt–BaO/Al_2O_3 lean NO_x trap material, no specific details regarding the amount of water and the treatment conditions were not given in the literature. In a subsequent study, Baiker and coworkers [14] demonstrated that bulk-like $BaCO_3$, which decomposes at high temperature, has a lower NO_x storage ability than smaller, poorly crystalline $BaCO_3$ species. In our previous work [13], we found that the degree of carbonation, i.e., crystallization of $BaCO_3$, was proportional to the water exposure levels. Thus, there remains the possibility of regenerating the NO_x storage activity by applying a minimal water treatment (e.g., to the incipient wetness level) to thermally aged samples, just sufficient to transform all Ba species in the $BaAl_2O_4$ phase into poorly crystalline $BaCO_3$, thereby restoring NO_x storage performance. The studies described here explore this possibility, and are aimed at identifying treatment conditions that regenerate $BaAl_2O_4$ without formation of large crystalline phases of $BaCO_3$.

2 Experimental

2.1 Preparation of Catalysts

$Ba(NO_3)_2$ was loaded on a high surface area gamma-alumina (Condea, 200 m^2/g, 0.57 cc/g pore volume) by repeated incipient wetness and drying at 120 °C under ambient conditions. $Pt(NH_3)_4(NO_3)_2$ was subsequently loaded onto the dried $Ba(NO_3)_2/Al_2O_3$ using incipient wetness impregnation and drying following similar procedures. The dried sample was calcined at 500 °C for 2 h in flowing air to decompose the precursors, which resulted in a sample containing 2 wt% Pt and 20 wt% BaO supported on Al_2O_3. Some samples were then treated under flowing 20% O_2/He or 20% H_2/He at 990 °C for 5 h. Catalysts to be discussed here are thus designated as Pt–BaO (as calcined, without treatment), Pt–BaO:O_2 (oxidative treatment) or Pt–BaO:H_2 (reductive treatment). These samples (as-calcined, O_2 aged, or H_2 aged) were treated with H_2O at the level of the incipient wetness (~0.5 cc/g) and designated as Pt–BaO–H_2O, Pt–BaO:O_2–H_2O, and Pt–BaO:H_2–H_2O, respectively. The H_2O treated samples were allowed to dry at room temperature overnight, then calcined at 500 °C, following the calcination procedure described above to remove the adsorbed water completely.

2.2 Reaction Tests

The reaction studies were carried out in a plug-flow quartz reactor system at atmospheric pressure, equipped with mass flow controllers and a 4-way valve with an electric actuator, simulating the compositions of lean and rich gases of diesel engine exhaust. Table 1 shows the composition of the cycled feed stream, which alternatively changes between oxidizing and reducing conditions. Each cycle consisted of a rich period for 1 min and a lean period for 4 min, and 4 cycles were carried out. The NO_x levels in the inlet (~200 ppm) and outlet gases were measured with a chemiluminescence NO_x analyzer (Thermo Environmental 42C). We used two ways to evaluate NO_x storage performance; short-term and long-term uptake. After performing four consecutive rich/lean cycles, NO_x concentrations were recorded while the catalyst was held for 30 min under an extended lean period. In this case, long-term NO_x uptake (%) is defined as the ratio of the total amount of NO_x stored to the total amount of inlet NO_x during this last 30 min lean

Table 1 Composition of the gas mixtures used during lean and rich period for LNT catalyst NO_x storage performance measurements

	Lean	Rich
NO	200 ppm	200 ppm
CO_2	10%	10%
H_2O	10%	10%
O_2	12%	0
H_2	0	1.33%
CO	0	4%
C_3H_6	0	1,330 ppm

Balanced with He

cycle after the 4th rich pulse. For the measurement of short-term NO_x uptake, the total amount of NO_x adsorbed up to 20% of inlet concentration (i.e., 40 ppm) from the beginning of the last lean period was obtained and normalized with catalyst weight (cm^3 (STP) NO adsorbed/g catalyst). The latter parameter indicates breakthrough behavior, with higher total NO_x uptake obtained when there is a longer breakthrough time. The flow rate of these simulated feed streams was kept at 300 cm^3/min and the weight of the catalyst in the powder form was 0.1167 g (gas hourly space velocity of 77,000 h^{-1}.). The gases leaving the reactor passed through the PERMA-PURE membrane to remove the water vapor before NO_x analysis by the CLA.

2.3 Characterization of Catalysts

Transmission electron microscopy (TEM) imaging was conducted on a JEOL 2010 high-resolution analytical electron microscope operating at 200 kV with a LaB_6 filament. The TEM instrument includes an energy dispersive X-ray (EDX) spectrometer. Powdered samples were dispersed in ethanol then mounted on copper grids containing a Formvar/carbon support film.

The X-ray diffraction (XRD) data were collected on a Philips X'Pert MPD (Model PW3040/00) with a vertical 2θ goniometer (190 mm radius). The X-ray source was a long fine-focus and sealed ceramic X-ray tube (Cu anode) operated at 40 kV and 50 mA (2,000 W). The optical train consisted of programmable divergence, anti-scatter, and receiving slits, incident and diffracted beam soller slits, a curved graphite diffracted beam monochromator, and a Xe-filled proportional counter detector. The diffraction data were analyzed using Jade 5 (Materials Data Inc., Livermore, CA) and the Powder Diffraction File database (International Centre for Diffraction Data, Newtown Square, PA).

3 Results and Discussion

3.1 Effect of Oxidizing or Reducing Conditions During the Thermal Aging on the Structural and NO_x Storage Properties

Figure 1 shows the XRD patterns for fresh and thermally aged Pt–BaO/Al_2O_3 samples treated under oxidizing and reducing conditions. The XRD of a BaO/Al_2O_3 sample calcined at 500 °C shows a diffraction pattern with peaks assignable only to the gamma (γ) Al_2O_3 support material. Ba containing phases in this sample (20 wt% loading) are not visible in the XRD, indicating that they are either amorphous or present as very small crystallites after calcination at 500 °C. The XRD invisible Ba phases are known to be nano-particulate BaO with ~5 nm average particle size, below the detection limit of conventional XRD, based on our previous high resolution synchrotron XRD experiments [15]. The subsequent heat treatment at an elevated temperature of 990 °C for 2 h, irrespective of oxidizing or reducing conditions, however, gives rise to formation of a crystalline $BaAl_2O_4$ phase, as evidenced from the appearance of multiple diffraction peaks in Fig. 1 that are characteristic of crystalline $BaAl_2O_4$ (PDF 82-2001). Although both samples contains several peaks arising from $BaAl_2O_4$, its average crystallite size, based on a peak-width analysis using the Scherrer equation, of the reduced sample is 95 nm, while that of the oxidized one is 55 nm, consistent with previous conclusions [7] that reducing treatments are much more effective than oxidizing ones in the formation of $BaAl_2O_4$.

In addition to the new $BaAl_2O_4$ phase, the XRD patterns of the high temperature treated samples (Fig. 1) demonstrate that, while the Pt–$BaO:O_2$ sample contains large Pt crystallites (about 80 nm based on peak profile analysis using the Scherrer equation), the Pt–$BaO:H_2$ sample contains no clearly evident peaks assigned to Pt metal. These results are in good agreement with previous reports [7] that the growth of crystalline Pt during thermal treatments is highly dependent on the oxygen concentration due to a high mobility of PtO_x species formed under oxidizing condition [16]. For the case of Pt–$BaO:H_2$, XRD peaks arising from crystalline Pt are barely, if at all detectable due, in part, to their overlap with the peaks (at $2\theta = 40, 46,$ and 67°) of $BaAl_2O_4$, which prevents a determination of the extent of Pt sintering from the XRD data. However, the representative TEM micrograph shown in Fig. 2(b) clearly demonstrates an increase in Pt particle sizes after H_2 treatment at 990 °C (note that TEM was not used to

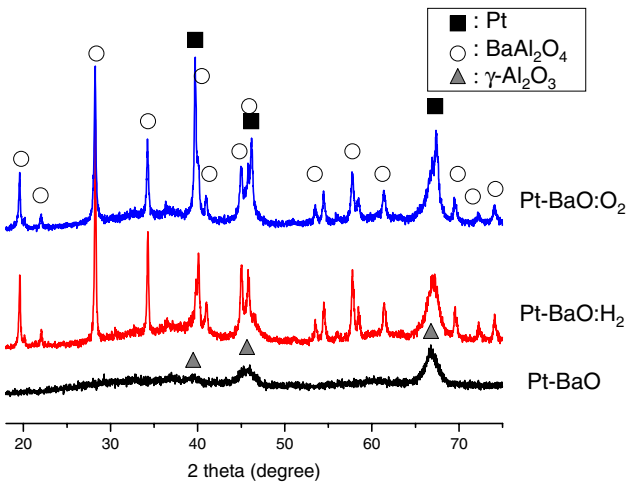

Fig. 1 XRD patterns of Pt–BaO, Pt–$BaO:H_2$, and Pt–$BaO:O_2$

estimate the Pt size in Pt–BaO:O_2 sample since XRD provides an accurate estimate of average particle sizes based on the sharpness of the diffraction peak(s).). For comparison, the Pt–BaO sample shows highly dispersed Pt clusters smaller than 2 nm (Fig. 2(a)), while the size of Pt increases to 2–10 nm for the case of Pt–BaO:H_2. It can, therefore, be summarized that an oxidizing environment promotes Pt sintering significantly, while reducing environments promote the transformation of Ba species to $BaAl_2O_4$ with relatively minor Pt crystallite growth observed.

As discussed above, because NO_x storage requires periodic desulfation processes carried out at elevated temperature in order to decompose thermodynamically stable $BaSO_4$, LNT catalysts are frequently exposed to thermal aging conditions that lead to Pt sintering and/or $BaAl_2O_4$ formation. These two phenomena were clearly evidenced in our just described results. To determine which deactivation mechanisms are primarily responsible for the decrease in NO_x storage capacity, Fig. 3 shows NO_x uptake over Pt–BaO/Al_2O_3 samples thermally treated under oxidizing or reducing conditions. Total NO_x uptakes up to the 20% breakthrough level (Fig. 3a), and for 30 min of lean operation (Fig. 3b) represent short-term and long-term NO_x uptake behavior, respectively. Pt–BaO:H_2 samples display, at most, a slightly lower NO_x uptake than the fresh Pt–BaO sample, but the uptake is severely reduced for the oxidized sample (Pt–BaO:O_2). Extremely low NO_x uptake for the Pt–BaO:O_2 sample can, in principle, be attributed to both of the formation of $BaAl_2O_4$ and the sintering of Pt. However, the fact that the Pt–BaO:H_2 sample, whose $BaAl_2O_4$ crystallites are even larger than Pt–BaO:O_2 based on the XRD results (Fig. 1), still maintains considerable NO_x uptake performance unambiguously demonstrates that NO_x uptake activity is more directly related to the severity of Pt sintering, rather than the formation of $BaAl_2O_4$. This result is in good agreement with our previous conclusions [17] that NO_x storage performance is inversely proportional to Pt particles size. Thus, it appears that the retention of small Pt particles during thermal aging is most crucial to the maintenance of NO_x uptake performance.

3.2 Effect of H_2O Treatment on the Structural and the NO_x Storage Properties

Figure 4 displays XRD patterns of variously treated Pt–BaO/Al_2O_3 samples after a final H_2O treatment. As we have previously reported for BaO/Al_2O_3 samples [13], the most significant change to the Pt–BaO:H_2–H_2O and Pt–BaO:O_2–H_2O samples upon water exposure is the appearance of XRD peaks from crystalline $BaCO_3$, replacing those due to $BaAl_2O_4$. Similar to these thermally aged samples, H_2O treatment of the calcined Pt–BaO sample induces a transformation of BaO to $BaCO_3$. Note that the crystallite sizes of the $BaCO_3$ phases (as determined by the Sherrer equation analysis of the width of the main $BaCO_3$ diffraction peak at 24°) are all in the 15–25 nm range for the three water treated samples, perhaps because we applied the same amount of water at the incipient wetness level for all three samples. In addition, there is no detectable change in the Pt XRD peak intensities at 40, 46, and 67° for all three samples. Therefore, the H_2O treatment does not affect the size of platinum particle, with the sole effect being the conversion of $BaAl_2O_4$ or BaO to $BaCO_3$.

As shown in Fig. 5, TEM micrographs taken for the water treated samples are fully consistent with the just described XRD results. In particular, a comparison of the TEM of the Pt–BaO–H_2O sample (Fig. 5a) with that obtained just after calcination of the fresh material (Fig. 2a) demonstrates that the size of Pt particles was not

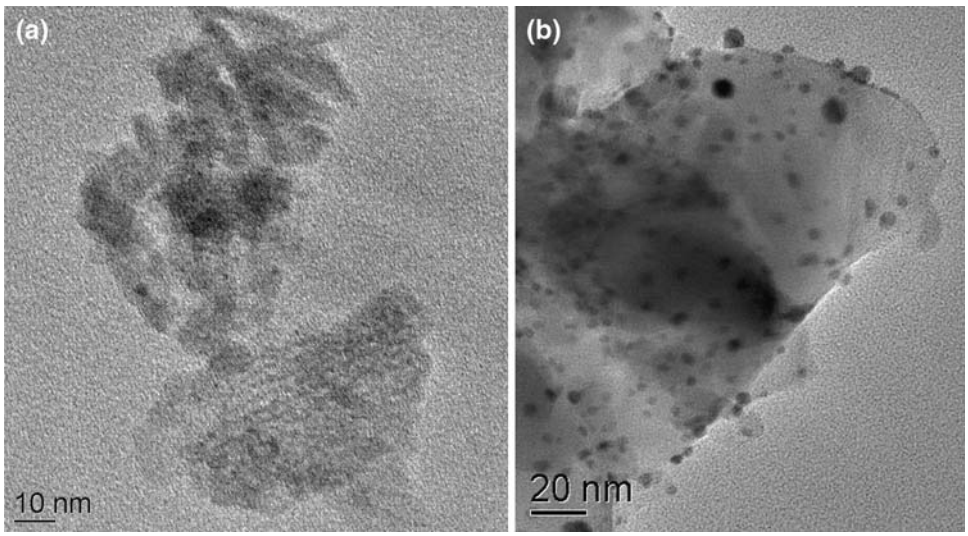

Fig. 2 TEM micrographs of Pt–BaO (**a**) and Pt–BaO:H_2 (**b**)

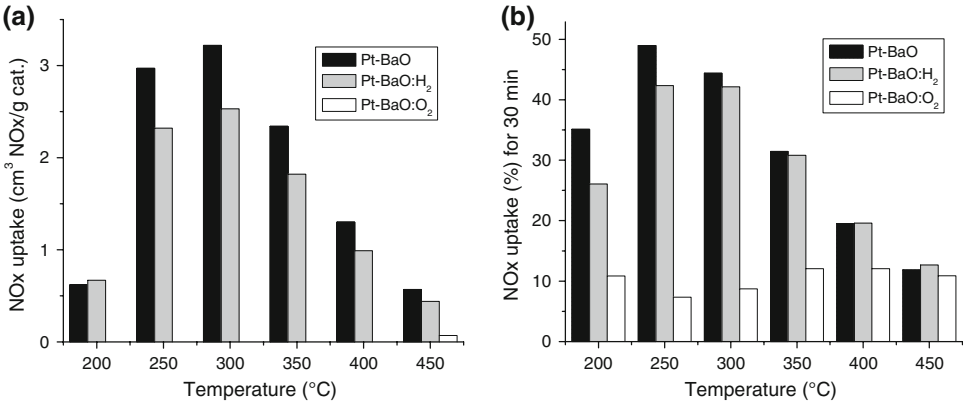

Fig. 3 NO_x uptake as a function of temperature: (**a**) up to 20% breakthrough of the inlet NO concentration, and (**b**) for 30 min over Pt–BaO, Pt–$BaO:H_2$, and Pt–$BaO:O_2$ catalysts

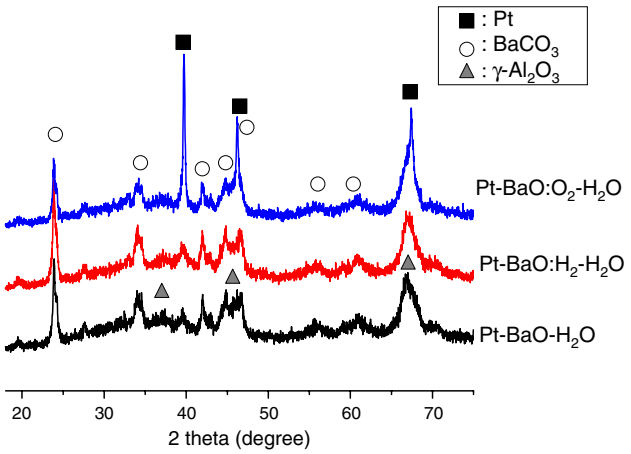

Fig. 4 XRD patterns of Pt–BaO–H_2O, Pt–$BaO:H_2$–H_2O, and Pt–$BaO:O_2$–H_2O

changed by the water treatment. A similar conclusion can be made with respect to Pt particle size changes in the Pt–$BaO:H_2$ samples before and after water treatment by comparison of the micrographs shown in Fig. 2b and Fig. 5b, respectively. However, it should be pointed out that, although the support matrix of Pt–$BaO:H_2$ in Fig. 2b is quite uniform (the dark area in the middle of the micrograph is due to sample thickness), the general catalyst morphology of the water-treated sample becomes inhomogeneous as marked in A and B in Fig. 5b. Areas A and B are rich in Al_2O_3 and $BaCO_3$, respectively. This result demonstrates that H_2O induced significant morphological changes in the BaO and/or Al_2O_3 components of the sample, in a good agreement with XRD results.

NO_x uptake activities for the three H_2O-treated samples are compared in Fig. 6. All three H_2O-treated samples show higher NO_x uptakes for short-term and long-term performance when compared to their non-treated counterparts (Fig. 3). Even the completely deactivated Pt–$BaO:O_2$ catalyst shows notable enhancement in both the short-term and long-term NO_x uptake performance. For the cases of the Pt–$BaO:O_2$–H_2O and Pt–$BaO:H_2$–H_2O samples, whose initial barium phases are $BaAl_2O_4$, the enhancement in NO_x uptake performance can be primarily explained by the phase change from $BaAl_2O_4$ to $BaCO_3$ since both XRD and TEM results displayed little, if any, change in Pt particle morphology. Such a significant increase in NO_x uptake after water treatment for both samples implies that the Ba phase change induced by water treatment is highly beneficial to NO_x storage.

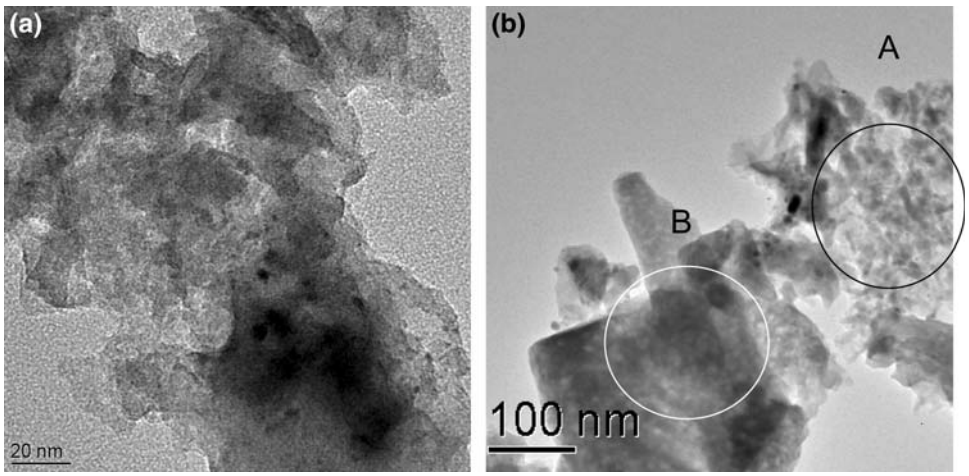

Fig. 5 TEM micrographs of Pt–BaO–H_2O (**a**) and Pt–$BaO:H_2$–H_2O (**b**)

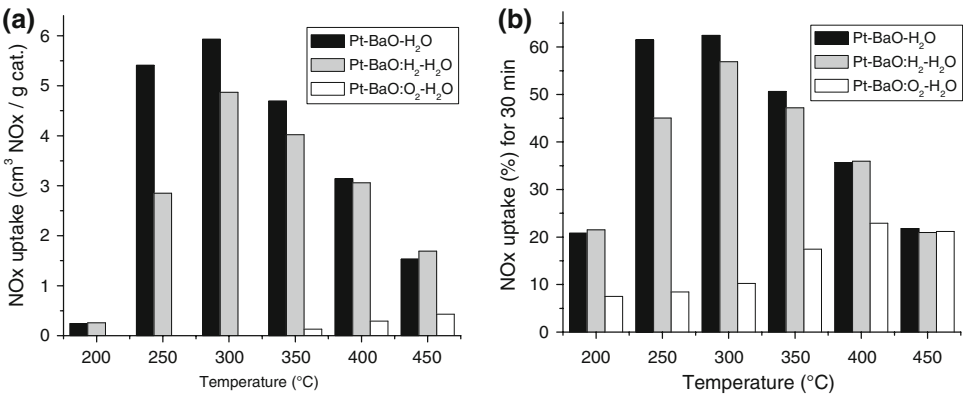

Fig. 6 NO_x uptake as a function of temperature: (**a**) up to 20% breakthrough of the inlet NO concentration, and (**b**) for 30 min over Pt–BaO–H_2O, Pt–BaO:H_2–H_2O, and Pt–BaO:O_2–H_2O samples

In addition, it is remarkable that freshly calcined Pt–BaO–H_2O sample exhibits short-term NO_x uptakes (Fig. 6a) almost twice that of the non-treated material (Fig. 3a) from 300 to 450 °C. In this case, the Ba phase changes cannot account for the increase in the activity because nano crystalline BaO rather than $BaAl_2O_4$ was the initially present Ba phase. In other words, a promotional effect of water treatment on NO_x storage is not limited to the thermally-aged samples containing $BaAl_2O_4$. Because there is no change in Pt particle sizes after water treatment as evidenced in the TEM results, the promotional effect of H_2O treatment can also not be explained by Pt morphology effects as was the case for reductions in reactivity of thermally aged samples. Instead, we propose that the observed enhancements upon water treatment can be explained by change in the proximity of Pt and Ba that promotes a synergistic interaction between these two LNT components. Consistent with this conclusion, TEM results demonstrated a morphological change in the Ba and alumina catalyst components resulting from the water treatment, which suggests a redistribution of barium species via the carbonation reaction. Such explanations are reasonable because an intimate Pt–Ba interaction [18, 19] has been regarded as a primary route to NO_x storage since NO_2, formed on Pt, may then readily spill over to the neighboring barium sites. Therefore, it can be summarized that the H_2O treatment at room temperature enhances the NO_x uptake for the fresh and thermally aged samples by promoting the Pt–BaO interaction through a redistribution of barium species on the LNT catalysts.

The impressive increase of NO_x uptake of the short-term lean period performance measurement upon water treatment (Fig. 6a) is especially worth mentioning. LNT catalysts that store more NO_x prior to significant breakthrough will require less frequent fuel-consuming rich periods during their operation, which can then lead to improvements in the overall fuel economy.

In our prior studies [13, 20] of the effects of water on thermally aged Pt–BaO/Al_2O_3 samples, we have shown that H_2O treatment transformed $BaAl_2O_4$ species into barium carbonate or barium nitrate depending on the presence or absence of NO_3^- ions on the sample. Here, we have shown that such morphology changes aid in recovering the NO_x storage activity for these thermally aged Pt–BaO/Al_2O_3 materials. Since water is always present in diesel engine exhaust, these results may well have practical implications for the operation of realistic systems. However, it must be emphasized that the amount of water is a key factor in the promotion (restoration) of NO_x storage performance. Overdosing water to the LNT catalysts can result in the formation of large $BaCO_3$ crystallites, which have been shown [7] to lead to a decrease in NO_x in contrast to the results presented here. Furthermore, the water vapor alone may not be sufficient to induce these beneficial Ba phase transformations as indicated by our prior results [13] that gas-phase water treatment at 125 °C did not lead to $BaCO_3$ formation.

4 Conclusions

XRD and TEM results presented here demonstrate that oxidizing treatments at 990 °C for Pt–BaO/Al_2O_3 catalysts causes significant sintering of Pt particles and the formation of $BaAl_2O_4$. On the other hand, reducing treatments at 990 °C lead to the formation of $BaAl_2O_4$ but, at most, minimal growth in Pt particle sizes. Liquid water treatments at the incipient wetness level for these samples promote the transformation of $BaAl_2O_4$ to $BaCO_3$ without altering the average sizes of Pt particles. In addition, we find that such water treatment for both fresh and thermally aged Pt/BaO–Al_2O_3 samples promotes NO_x uptake and storage. These enhancements in NO_x uptake after treating the sample with water are primarily attributed to a promotion of Pt–Ba contact caused by morphological and structural rearrangements (including migration) of the barium species. These results suggest possible practical strategies for regenerating thermally aged LNT catalysts

utilizing abundantly present water in the exhaust of diesel and other lean-burn engines.

Acknowledgment Financial support was provided by the U.S. Department of Energy (DOE), Office of Energy Efficiency and Renewable Energy, Vehicle Technologies Program. The work was performed in the Environmental Molecular Sciences Laboratory (EMSL) at Pacific Northwest National Laboratory (PNNL). The EMSL is a national scientific user facility and supported by the U.S. DOE, Office of Biological and Environmental Research. PNNL is a multi-program national laboratory operated for the U.S. Department of Energy by Battelle Memorial Institute under Contract DE-AC06-76RLO 1830.

References

1. Takahashi N, Shinjoh H, Iijima T, Suzuki T, Yamazaki K, Yokota K, Suzuki H, Miyoshi N, Matsumoto S, Tanizawa T, Tanaka T, Tateishi S, Kasahara K (1996) Catal Today 27:63–69
2. Epling WS, Campbell LE, Yezerets A, Currier NW, Parks JE (2004) Catal Rev-Sci Eng 46:163–245
3. Engstrom P, Amberntsson A, Skoglundh M, Fridell E, Smedler G (1999) Appl Catal B-Environ 22:L241–L248
4. Amberntsson A, Skoglundh M, Ljungstrom S, Fridell E (2003) J Catal 217:253–263
5. Lietti L, Forzatti P, Nova I, Tronconi E (2001) J Catal 204:175–191
6. Jang BH, Yeon TH, Han HS, Park YK, Yie JE (2001) Catal Lett 77:21–28
7. Graham GW, Jen HW, Chun W, Sun HP, Pan XQ, McCabe RW (2004) Catal Lett 93:129–134
8. Fridell E, Persson H, Westerberg B, Olsson L, Skoglundh M (2000) Catal Lett 66:71–74
9. Li J, Theis JR, Chun W, Goralski C Jr, Kudla R, Ura J, Watkins W, Chattha M, Hurley R SAE paper (2001-01-2503)
10. Hodjati S, Bernhardt P, Petit C, Pitchon V, Kiennemann A (1998) Appl Catal B-Environ 19:209–219
11. Hodjati S, Bernhardt P, Petit C, Pitchon V, Kiennemann A (1998) Appl Catal B-Environ 19:221–232
12. Graham GW, Jen HW, Theis JR, McCabe RW (2004) Catal Lett 93:3–6
13. Kim DH, Chin YH, Kwak JH, Szanyi J, Peden CHF (2005) Catal Lett 105:259–268
14. Piacentini M, Maciejewski M, Baiker A (2005) Appl Catal B-Environ 60:265–275
15. Szanyi J, Kwak JH, Hanson J, Wang CM, Szailer T, Peden CHF (2005) J Phys Chem B 109:7339–7344
16. Datye AK, Xu Q, Kharas KC, McCarty JM (2006) Catal Today 111:59–67
17. Kim DH, Chin YH, Muntean GG, Yezeretz A, Currier NW, Epling WS, Chen HY, Hess H, Peden CHF (2006) Ind Eng Chem Res 45:8815–8821
18. Cant NW, Liu IOY, Patterson MJ (2006) J Catal 243:309–317
19. Kwak JH, Kim DH, Szailer T, Peden CHF, Szanyi J (2006) Catal Lett 111:119–126
20. Kim DH, Kwak JH, Szanyi J, Burton SD, Peden CHF (2007) Appl Catal B-Environ 72:233–239